# pH sensitive composite hydrogels based on gelatin and reinforced with cellulose microcrystals: In depth physicochemical and microstructural analyses for controlled release of vitamin B2

Soumaya Boughriba, Nabil Souissi, Rim Nasri, Moncef Nasri, Suming Li

# pH sensitive composite hydrogels based on gelatin and reinforced with cellulose microcrystals: In depth physicochemical and microstructural analyses for controlled release of vitamin B2

Soumaya Boughriba [a,b], Nabil Souissi [c,*], Rim Nasri [a,d], Moncef Nasri [a], Suming Li [b]

[a] Laboratory of Enzyme Engineering and Microbiology, University of Sfax, National Engineering School of Sfax, 3038 Sfax, Tunisia
[b] Institut Européen des Membranes, IEM-UMR 5635, Univ Montpellier, ENSCM, CNRS, 34095 Montpellier, France
[c] Laboratory of Marine Biodiversity, National Institute of Marine Sciences and Technologies, University of Carthage, Tunisia
[d] National Institute of Biotechnology of Monastir, Avenue Taher Hadded (B.P 74), Monastir 5000, Tunisia

*Keywords:*
Hydrogels
Gelatin
Cellulose microcrystals
Drug controlled delivery

The aim of this work was to develop pH sensitive composite hydrogels based on *Rhinobatos cemiculus* gelatin (RCG) and reinforced with cellulose microcrystals (CM) for vitamin B2 controlled release. Hydrogels were synthesized using different CM ratios. The structure and stability of the prepared hydrogels were determined using FTIR, SEM, DSC and TGA analyses. The presence of CM effectively improved the mechanical properties, the resistance to thermal degradation, and the compactness of composite hydrogels, as evidenced by rheological and dynamic mechanical tests. Moreover, the pore size decreased and became more regular with the increase of CM content. Additionally, RCG hydrogels loaded with 5% of CM, in acidic medium, underwent higher swelling rate, compared to other hydrogels in neutral and basic media. Hydrogels' porous microstructure and swelling behavior were determining parameters in riboflavin entrapment efficiency and controlled release rate. This supplied flexible choices for the development of drug carrier for controlled delivery.

## 1. Introduction

To normally and safely fulfill its essential functions, the human body requires a certain amount of components including vitamins and minerals in adequate quantities. Such nutrients improve body resistance immune system regarding their roles on normal growth while assisting cells and organs for a best performance [1], whereas their deficit could lead to serious diseases. Riboflavin, also referred to as vitamin B2, is considered as essential vitamin for human and animal health. It is also produced biotechnologically as food supplement due to its role in energy survival through distinguished function in human body as a key molecule in the aerobic metabolism of amino acids and fatty acids [1,2]. Moreover, riboflavin is gaining an increasing interest since it is a precursor for Flavin cofactors which are commonly used as intrinsic biomarkers for cellular bioenergetics [3,4]. A recent study [5] mentioned that the daily recommendation for dietary riboflavin is 1.6 mg and 1.2 mg for male and female, respectively. With such a respectful dietary in riboflavin, Humans will prevent headaches including migraines, anemia and will provide constant level of energy and ensure the body from oxidation damages since it is also known as antioxidant component [1,6].

Sustained release systems have been extensively studied in the past decades as they allow to attain tunable drug release with enhanced efficiency, reduced side effects and upgraded patient compliance [7]. In fact, a constant release rate is of crucial importance to minimize the fluctuation of drug concentration in plasma with respect of its minimum effective concentration and maximum safe concentration [8]. Much attention has been devoted to hydrogels as drug carrier thanks to their superior biological as well as physicochemical features. Hydrogels are composed of a three-dimensional (3D) network based on hydrophilic polymers which is able to retain large amount of water or biological fluids, while maintaining their 3D architecture [9,10]. Moreover, hydrogels can ensure both degradability and targeted behavior as a response to various stimuli such as temperature, pH or ionic strength, leading to the release of the entrapped drug in a controlled manner [11–13]. Several triggered responsive hydrogels, known as smart hydrogels have been widely discussed in the literature, regarding their ability to adjust the drug delivery profile for self-regulated or pulsed

* Corresponding author at: INSTM, Avenue Madagascer, BP 1035, 3018 Sfax, Tunisia.
*E-mail address:* nabil.souissi@gmail.com (N. Souissi).

mechanism [14].

Biopolymers are commonly employed as raw materials for the development of drug delivery systems due to their outstanding properties including non-toxicity, biocompatibility and safety [15–17]. Among them, gelatin, a protein derived from partial hydrolysis of collagen in either acidic (type A) or alkaline (type B) conditions [18], attracted much interest for synthesizing smart hydrogels thanks to its physico-chemical and biological features, including relatively low cost, biodegradability, high water absorbance, cell adhesion capacity, low immunogenic, uncomplicated chemical modification and cross-linking due to accessible moieties which are mainly hydroxyl, carboxyl and amine groups [19–22].

Literature evidence suggests that polysaccharide chains and gelatin are habitually used together to form hydrogels in the presence of glutaraldehyde which reacts with the amino group of gelatin to form a Schiff base structure covalently connecting gelatin molecules and followed by polysaccharide chains non-covalently crosslinked with gelatin by establishing hydrogen bonds. Consequently, a 3-dimensional mesh structure will be obtained with high resistance to heat, preventing as a result its dissolution at human body temperature and promoting its application in biomedical field. However, glutaraldehyde is used in some medical treatments, especially those related to dental treatment as a part of the technique for bonding a restoration, after etching [23]. Additionally, the ocular and dermal irritancy of this reagent could be significantly avoided if its concentration did not exceed 0.5 % with a brief and discontinuous exposure [24]. It has been reported that non-uniform crosslinking could occur during the hydrogel formation [25], which is not beneficial for the applications of gelatin. Other polymers have been introduced into the gelatin network to prepare composite hydrogels, including cellulose nanofibrils [26], glucomannan [27], etc. In a recent study, it has been shown that most bio-polymeric composites are suitable for drug delivery as they display advanced properties in comparison to pure biopolymers [28]. Cellulose, as the most abundant biopolymer has been used for various applications in the biomedical field [29]. The microcrystalline form of cellulose, which is a commercially available material obtained by acid hydrolysis of cellulose [30], has been applied as a filler in different composites since it contains abundant hydroxyl groups involved in the formation of hydrogen bonds. Microcrystalline cellulose has been successfully used to form composite hydrogel beads using chitosan, carrageenan, agarose and agar [31]). The non-toxicity, low density, high mechanical strength, large surface area, biodegradability and biocompatibility of cellulose microcrystals allowed uses as adsorbents, thickeners and binders in pharmaceutical and cosmetic industries; stabilizers, gelling agents and anticaking agents in food and beverage industries [32]. The novelty in this study lies in the design of a material based on newly extracted polymer from a fish skin, which is gelatin, in order to use it in biomedical application. Precisely, the proposed technology provides a drug delivery system which employed a biopolymer based hydrogel to deliver riboflavin in response to a pH variation. The objective of this work was to develop fish gelatin-based hydrogels, and to assess the effect of microcrystalline cellulose addition on the structural, thermal, mechanical and rheological properties of the resulting composite hydrogels. Subsequently, riboflavin was loaded in composite hydrogels to evaluate the drug delivery performance in terms of drug encapsulation efficiency, loading capacity and release profile.

## 2. Materials and methods

### 2.1. Materials

The model drug, Riboflavin, is supplied by LOBA CHEMIE (India). Cellulose microcrystals (Avicel PH101, 50 μm) were purchased from Fluka. Glutaraldehyde (Grade II, 25 % in H2O) was obtained from Sigma Aldrich. Fish gelatin was extracted from the skin of *Rhinobatos cemiculus* and characterized [33], to be used in the present study. All other chemical reagents were of analytical grade and used as received.

### 2.2. Conception of gelatin-microcrystalline cellulose composite hydrogels

The preparation of RCG-CM hydrogels was carried out as follows. First, aqueous dispersions of cellulose microcrystals (CM) were prepared in deionized water and homogenized using continuous ultra-sonication. Gelatin was then added to the CM suspension which was stirred at 50 °C for 1 h, yielding a homogenous viscous mixture. Afterwards, 0.3 % of glutaraldehyde were added dropwise, and the mixture was gently stirred for 4 h to prevent bubble formation. The resulting hydrogels were then washed 3 times in PBS for 15 min each. Subsequently, the hydrogels were immersed in sterile-filtered glycine solution (0.1 M) under constant shaking overnight to neutralize any residual glutaraldehyde. Finally, the hydrogels were washed two more times in sterile PBS for 15 min each, and then dried in an oven at 37 °C up to constant weight. The compositions of the prepared RCG-CM hydrogels vary in terms of CM added amount (5%, 10 %, 15 %, 20 % and 25 %) which is presented on the base of dry weight of added gelatin.

### 2.3. Characterization

#### 2.3.1. Fourier transform infrared spectroscopy

Fourier transform infrared (FTIR) of freeze dried samples was performed with a spectrometer (Thermo Fisher Scientific, Model: Nexus) with an attenuated reflectance accessory (ATR) equipped with a diamond crystal. Spectra were recorded in the 4000 to 600 $cm^{-1}$ wavenumber range with 4 $cm^{-1}$ resolution and 32 scans of interferograms. The obtained data were treated using the OMNIC Spectra software (Thermo Fisher Scientific).

#### 2.3.2. Scanning electron microscopy

The microstructure of RCG-CM hydrogels' cross section was examined using scanning electron microscope (Hitachi S4800). Prior to imaging, lyophilized samples were sectioned and sputter coated with a thin gold layer. An accelerating voltage of 2.0 kV was used with a High Mag Mode 100 x magnification.

#### 2.3.3. Swelling of hydrogels

Typically, samples of dried hydrogels (40–50 mg) were immersed in different buffer solutions ranging from pH 2 to pH 10 at room temperature in order to determine the equilibrium swelling ratio of RCG-CM hydrogels. After 24 h, samples were taken out from the solution, weighed after removing the surface buffer using a filter paper, freeze-dried for 24 h, and weighed again. Experiments were performed in triplicate. The swelling ratio (SR) was calculated as according to the following formula:

$$\mathrm{SR}(\%) = \frac{Ws - Wd}{Wd} \times 100$$

Where Ws is the wet weight of the swollen hydrogel, and Wd is the dried weight of after lyophilization

#### 2.3.4. Rheological properties of hydrogels

Rheological measurements of RCG-CM hydrogels were carried out with a rheometer (Physica MCR, Anton Paar, GmbH, France) using a plate-plate measuring cell (25 mm diameter, 0.1 mm gap). The storage modulus (G′) and loss modulus (G″) were determined under angular frequency sweep from 0.1–100 rad/s at 37 °C and a strain of 1%. The resulting data were analyzed with Rheoplus software from Anton Paar.

#### 2.3.5. Mechanical properties of hydrogels

Compression experiments were performed on RCG-CM hydrogels using the DMA50 Dynamic Mechanical Analyzer universal testing apparatus (Metravib, Brand of ACOEM, France) at a compression speed

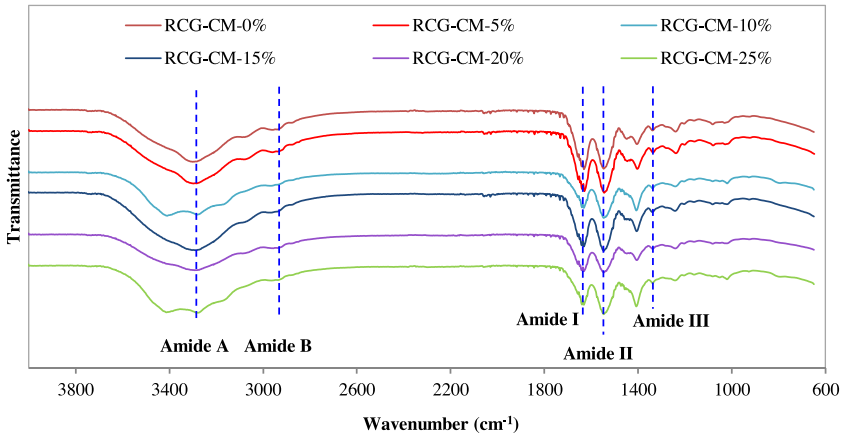


**Fig. 1.** ATR-FTIR spectra of RCG hydrogels added with different percentage of cellulose microcrystals.

of 1 mm/min and at 25 °C. Cylindrical hydrogel samples (10 mm in diameter and 10 ± 1 mm in height) were used for all experiments. Samples were compressed at different levels (10 %, 20 %, 30 %, 40 % and 50 %), and then recovered at the same speed of 1 mm/min. The compression-recovery cycles resulted in stress-strain curves.

### 2.3.6. *Thermal properties of hydrogels*

Differential scanning calorimetry (DSC) was performed with DSC Q20 (TA Instruments) equipped with a liquid nitrogen cooling unit. Prior to analysis, RCG based hydrogels were heated from room temperature to 200 °C to remove the adsorbed moisture. After 2 min at 200 °C, samples were cooled down to room temperature, and then the heat flow variation was analyzed in the 20–250 °C temperature range. Nitrogen purge was applied at a 50 mL/min flow rate. All heating and cooling steps were performed at 10 °C/min. The obtained DSC thermograms were analyzed using TA Universal Analysis 2000 software (version 4.5 A, TA instruments).

Thermogravimetric analysis (TGA) was carried out using TGA Q500 High Resolution (TA Instruments) to evaluate the thermal stability of RCG based hydrogels. 5 mg of each sample were heated from 25 to 700 °C at a heating rate of 20 °C/min. The resulting thermograms were analyzed using TA Universal Analysis 2000 software (version 4.5 A).

### 2.3.7. *In vitro drug release*

Riboflavin loading in hydrogels was performed based on the swelling-diffusion method. Briefly, 50 mg of each hydrogel sample was immersed in 10 mL of riboflavin solution (3 g/l) for 48 h, maintained in dark at 4 °C. The hydrogel was then removed from the solution. The remaining free riboflavin in solution was determined using a UV–vis spectrophotometer JENWAY 7315 at 450 nm. A calibration curve was previously established from a series of riboflavin solutions at different concentrations. The riboflavin encapsulation efficiency (EE) and loading capacity (LC) were determined as follows:

$$\textbf{Entrapment efficiency (EE)} = \frac{\textit{weight of the loaded riboflavin}}{\textit{weight of initial riboflavin}} \times 100$$

$$\textbf{Loading capacity (LC)} = \frac{\textit{weight of the loaded riboflavin}}{\textit{weight of hydrogel sample}} \times 100$$

Riboflavin loaded hydrogels were placed in a flask containing 10 mL of PBS adjusted to pH 2 and pH 7.4. Drug release was performed at 37 °C under continuous stirring. 3 mL of the release medium was collected at each time interval and replaced with 3 mL of fresh PBS to preserve constant volume. The concentration of riboflavin in the solution was determined using UV–vis spectrophotometer JENWAY 7315 at 450 nm.

## 3. Results and discussion

### 3.1. *Fourier transform infrared analysis*

Fig. 1 shows the FTIR spectra of RCG and RCG-CM composite hydrogels. RCG hydrogel presents a C═O stretching band at 1634 $cm^{-1}$ (amide I), N—H bending band at 1538 $cm^{-1}$ (amide II), C—N stretching band (amide III) at 1238 $cm^{-1}$ and A band at 3280 $cm^{-1}$. These bands are also detected in the spectra of RCG-CM composite hydrogels. Nevertheless, peaks of amide I, II and III in RCG-CM hydrogels slightly upshifted as compared with those of the RCG hydrogel. In fact, the

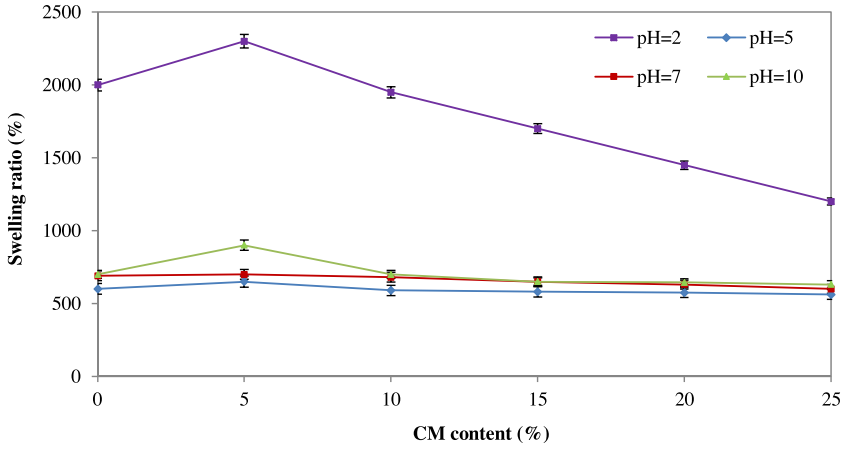


**Fig. 2.** Swelling ratio of different cellulose microcrystals –gelatin hydrogels at various pH values.

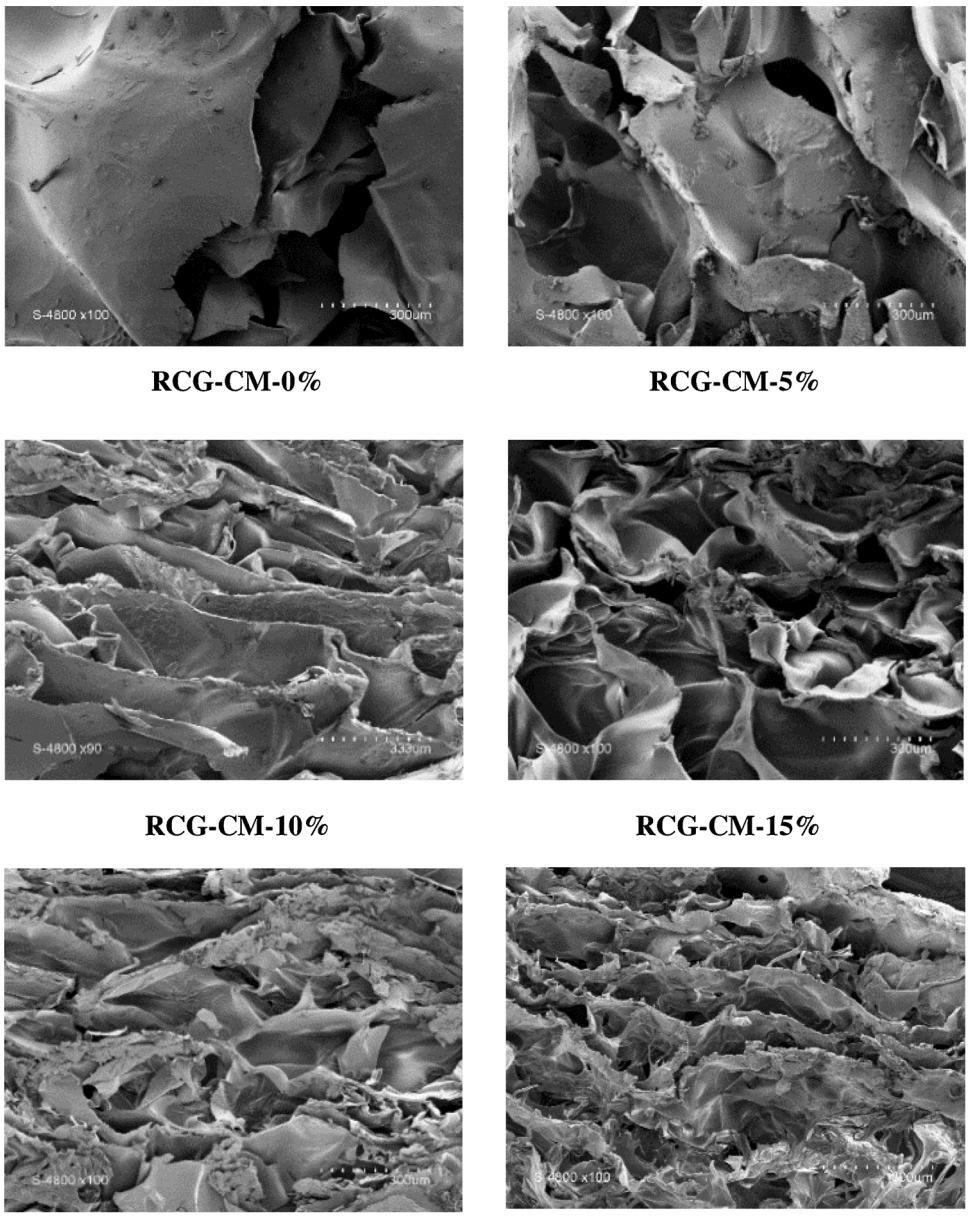


**Fig. 3.** SEM micrographs of cross section of RCG hydrogels added with different percentage of cellulose microcrystals.

vibrational frequency of C═O band of amide I is affected by the hydrogen bonding between amide units [34], the slight frequency shift of amide I peaks in the RCG-CM hydrogel reflects the interruption of hydrogen bonds at carbonyl groups of gelatin [35] by competitive bonding of CM. Thus, the polarity could decrease as more hydrogen bonds are formed between gelatin and CM. Yakimets et al. [36] reported that the addition of cellulose decreased the hydration due to competitive binding to water molecules, resulting in the antiplasticizing effect. In addition, the shift in amide I, II and III bands may be attributed to a protein dilution effect [35] resulting from the partial replacement of gelatin by CM and the amide-cellulose interactions initiating conformational changes. Moreover, the peak appearing at 1160 $cm^{-1}$ may be attributed to the antisymmetric bridge stretching of C—O—C groups in cellulose as mentioned by Cao and Tan [37]. Therefore, it can be concluded that the enhanced properties of RCG-CM hydrogels result from the hydrogen bonds which increase the hydrophobic nature of the gelatin- cellulose microcrystals matrix.

### 3.2. *Equilibrium fluid uptake of hydrogels*

Hydrogels can be used for biomedical applications depending on their swelling behavior which reflects the body fluid uptake and nutrient penetration within the scaffolds [38,39]. Thus, swelling is an important indicator allowing to better understand the structure of hydrogels which is strongly related to several parameters such as network density, hydration ability of materials, ion strength and pH [40].

The effect of both CM concentration and pH variation on the swelling ratio (SR) of RCG based hydrogels was investigated. As shown in Fig. 2, the hydrogels displayed similar fluid uptake patterns for all pH values. Interestingly, an increase in swelling ratio was observed with 5% CM hydrogel, which may be attributed to the hydrophilic character of CM [41]. When the concentration of CM exceeds 5%, however, the swelling

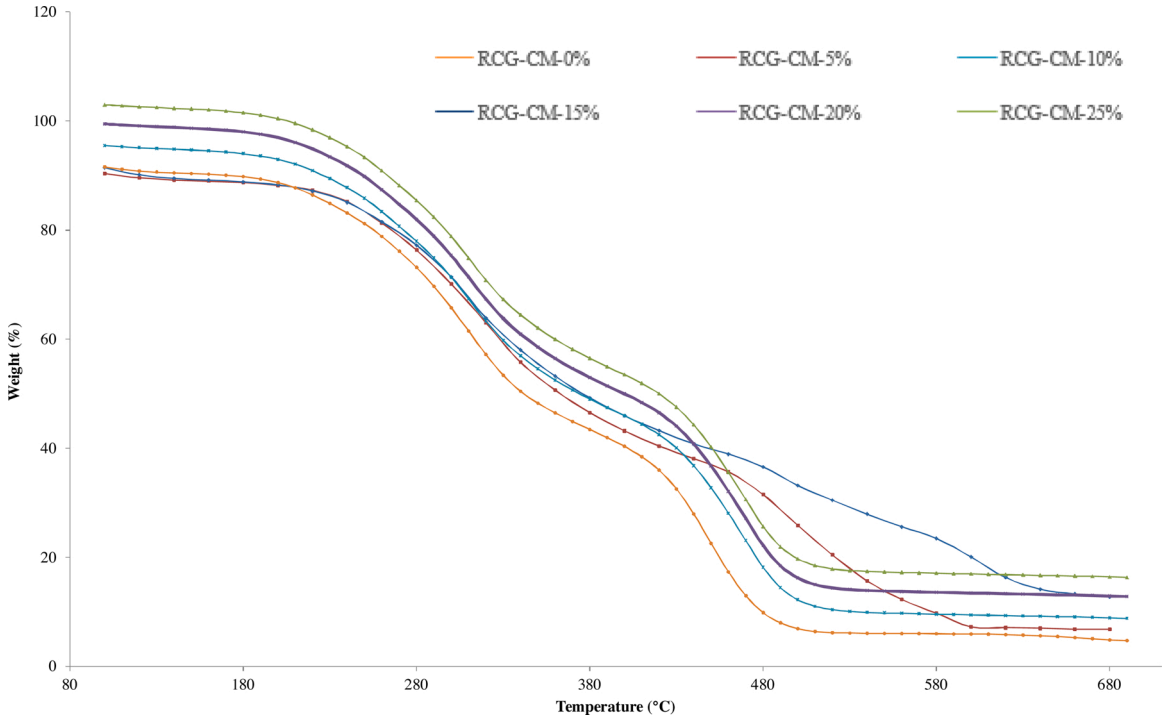


**Fig. 4.** TGA thermograms of weight loss of RCG hydrogels added with different percentage of cellulose microcrystals.

ratio of hydrogels gradually decreased. The possible reason is that the increase in CM concentration enhances the crosslinking density and reduces the network voids, leading to a decrease in fluid uptake. Therefore, the lowest SR value is observed for the composite with the highest CM concentration. These results are in accordance those reported by Gu et al. [42]. The authors observed that with increase of cellulose particles content in the gelatin hydrogel network, more hydrogen bonds were formed restricting thus the hydrogel swelling. The swelling behavior was monitored at pH values ranging from 2 to 10 in order to simulate the condition of gastric and intestinal microenvironments. In acidic environment, RCG-CM hydrogels exhibited slightly higher swelling compared to the basic environment. This finding was attributed to the polyelectrolyte character of gelatin that makes it an amphoteric polymer whose degree of ionization is sensitive to the pH of the medium owing to the presence of carboxyl and amino acid groups [43]. In fact, gelatin contains amino groups in its structure which are protonated in acidic medium, creating electrostatic repulsions leading to a rise of swelling ratio. However, in basic medium, carboxyl acids are deprotonated, the electrostatic repulsion is thus decreased, leading to a decrease of swelling [44,45]. On the other hand, the isoelectric point (pI) of RCG was about 5 as mentioned in our previous study [33]. Thus, hydrogels placed at this pH would have a zero net charge since the number of negative charges is equal to that of positive charges. This ionic state will generate strong attractions between opposite charges leading to a dense network with the lowest swelling. Therefore, the swelling of RCG-CM hydrogels is sensitive to pH variation in the range of 2−10. At 5% of CM, the polymeric network presents the maximum of swelling. Additionally, the swelling degree of all hydrogels appears asymmetric around the isoelectric point with higher swelling when charged positively (below pI) than negatively (above pI), in agreement with literature [46,47].

### 3.3. Morphological structure of hydrogels

Fig. 3 shows the microstructure of gelatin hydrogels with and without CM. Gelatin hydrogel without CM showed a very loose structure with large pores and smooth walls, while CM loaded hydrogels exhibited a more compact structure with smaller pores, suggesting that the porosity decreased with increasing CM content. This finding can be explained by the fact that incorporation of CM effectively led to the formation of a rigid hydrogel structure. As the hydrogel become stiffer, the equilibrium swelling ratio decreases and thus reduces the pore size as described by Yin et al. [41]. Additionally Kim and Chu [48] and Liao et al. [49] demonstrated in their studies that the addition of cellulose fillers in gelatin hydrogels guaranteed more intermolecular association through a large number of gelatin-cellulose junction points affecting thus the pore distribution and size. In other studies, the use of cellulose as filler in gelatin hydrogel was shown to decease the pore size and to improve shape regularity of the gelatin hydrogel [41]. Thus the concentration of CM has to be optimized to obtain the adequate pore size distribution needed to make the gelatin matrix a good three dimensional network for cell encapsulation or drug delivery.

### 3.4. Thermogravimetric analysis

The thermal behavior of hydrogels is governed by the thermo-responsive mechanism of the crosslinked three dimensional network (Rocha-García et al. [50]). Hence, TGA was performed to better understand the thermal decomposition behavior of RCG-CM hydrogels, as shown in Fig. 4. All RCG-CM hydrogels showed similar patterns with a continuous weight loss up to 700 °C, reflecting the typical fingerprint of both gelatin and cellulose decomposition. The weight loss curves can be divided into three phases. The first phase displayed a minor weight loss in the temperature range up to 200 °C, corresponding to the removal of entrapped water molecules in the hydrogel network [51]. More precisely, different onset temperatures were detected for hydrogels reflecting the different contents of bound and unbound water in the hydrogels [52]. Additionally, RCG-CM-0% hydrogel was found to exhibit the lowest onset temperature probably due to more unbound water as evidenced by SEM micrographs. In contrast, CM loaded hydrogels displayed higher onset temperature, suggesting the presence of more bound water associated to a more homogeneous network structure [53].

For the second phase, a significant weight loss was observed in the

**Table 1**
Thermal transitions in terms of glass transition temperature, melting temperature and melting enthalpy of RCG hydrogels added with different percentage of cellulose microcrystals.

| Samples | $T_g$ (°C) | $T_m$ (°C) | $\Delta H_m$ (J/g) |
|---|---|---|---|
| RCG-CM-0% | 48.9 | 115.3 | 91.3 |
| RCG-CM-5% | 50.3 | 107.5 | 96.5 |
| RCG-CM-10 % | 50.5 | 112.8 | 148.5 |
| RCG-CM-15 % | 55.0 | 113.9 | 179.2 |
| RCG-CM-20 % | 56.2 | 113.4 | 217.1 |
| RCG-CM-25 % | 61.2 | 112.6 | 239.7 |

temperature range of about 200–400 °C, indicating the thermal decomposition of glucose units of cellulose or peptide chains of gelatin [54–56]. When compared with other composite hydrogels, RCG-CM-25 % hydrogel possessed higher residue content, proving a better thermal stability as a result of a uniform and moderate CM distribution in the hydrogel structure [57]. In fact, a strong intermolecular linking requires more bond dissociation energy to cleave chains constituting the network [58]. Subsequently, a well-dispersed CM and a good interfacial adhesion between CM and polymer matrix are required for the development of thermally stable hydrogels [59]. In contrast, for other composite hydrogels lower residues were observed, reflecting lower thermal stability that could be caused by the high surface area of CM, which led to a larger exposure to heat and the partial interruption in the cellulose crystal structure [60]. Thus the thermal stability of RCG hydrogels can be improved by incorporation of well distributed CM.

Similar findings were reported by Siangsanoh [57]. The authors showed that cellulose is responsible for the thermal stability of gelatin hydrogel due to its uniform distribution in the hydrogel structure. The third phase referred to the decomposition of remaining materials at the temperature higher than 400 °C, probably resulting from the cross-linking reaction between gelatin chains and glutaraldehyde [57]. Precisely, at a temperature higher than 400 °C, the weight loss decreased slowly for RCG-CM-5% and RCG-CM-15 % in a different manner compared to the remaining hydrogels. This tendency could be explained by the fact that when the hydrogel formulation contained 5% of CM, the crosslinking was in favor of covalent bonds between protein chains via glutaraldehyde and as a result, the thermal stability increased and a decrease of the weight loss value was observed. On the other hand, when the concentration of CM in the hydrogel formulation increased and reached 15 % the degradation of protein chains was no longer the major process and thus the hydrogels decompose in a slower manner. Additionally, the residual weight at 700 °C, ranging from 5% to 18 %, was found to rise as the CM content increased from 0% to 25 %. This could be attributed to the crosslinking bonds occurred between CM and gelatin chains, creating therefore a reticulate structure and as a result the residual weight increased. This could indicate that the CM with the characteristic of stable structure were found to enhance the compactness of RCG hydrogels and to slightly retard the thermal decomposition of gelatin.

### 3.5. *Differential scanning calorimetry analysis*

The thermal transition profiles of all developed hydrogels was studied through DSC analysis, which allowed to draw supplementary evidences about the hydrogels composition [61]. Based on DSC results, the glass transition temperature (Tg) of the neat RCG hydrogel (RCG-CM-0%) was around 49 °C (Table 1). However, the Tg of the CM added RCG hydrogels slightly increased as the CM concentration increased to attain its maximum of almost 61 °C for RCG-CM-25 %. Hence, the added amount of CM that was incorporated within the system was proved to slightly affect the glass transition temperature. This finding suggested that the incorporation of the cellulose microcrystals did not hinder the molecular motion of the gelatin chains from the glassy state to the rubbery state. In addition, the melting temperature of gelatin based hydrogels was found to slightly vary when CM were added. The melting enthalpy, which reflects the energy required to disrupt the cross-linked junction zones [62], displayed also an increasing tendency reflecting hydrogels' thermostability. This may be due to the establishment of stronger junction zones or to a rise in the number of junction zones as much as the CM content increases. Taken all together, it would be rational to suppose that RCG-CM hydrogels displayed a thermally stable structure.

### 3.6. *Compression testing*

Compression tests were performed considering the asset of microcrystals to improve the dynamic mechanical behavior of a large variety of biomaterials like hydrogels [63]. The typical stress *vs.* strain compressive curves are shown in Fig. 5. Results show that under compression, the compressive strength of the RCG-CM hydrogel samples increased with the increase in strain for all hydrogel formulations. Precisely, the compressive stiffness of RCG-CM hydrogels increases alongside with that of the applied compressive strain in the range of 1–6 %, followed by a slower increase, indicating that the RCG-CM hydrogels are typically ductile materials. On the other hand, the ultimate fracture strain of the hydrogels increased with the increase of CM concentration. In fact, CM free hydrogels displayed an ultimate strain of 32 % against 44 % for RCG hydrogels loaded with 25 % of CM, indicating that the fracture strain of gelatin based hydrogels was improved by the introduction of CM. However, the hydrogel's breaking stress was found to

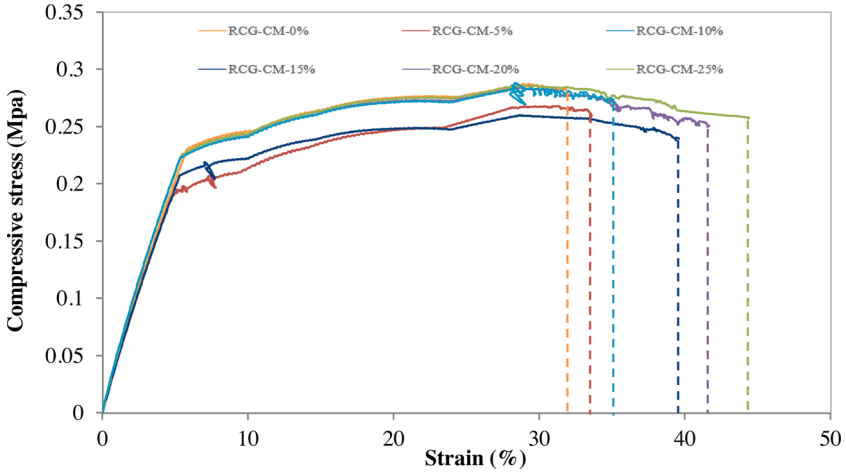


**Fig. 5.** Compressive stress-strain curves of RCG hydrogels added with different percentage of cellulose microcrystals.

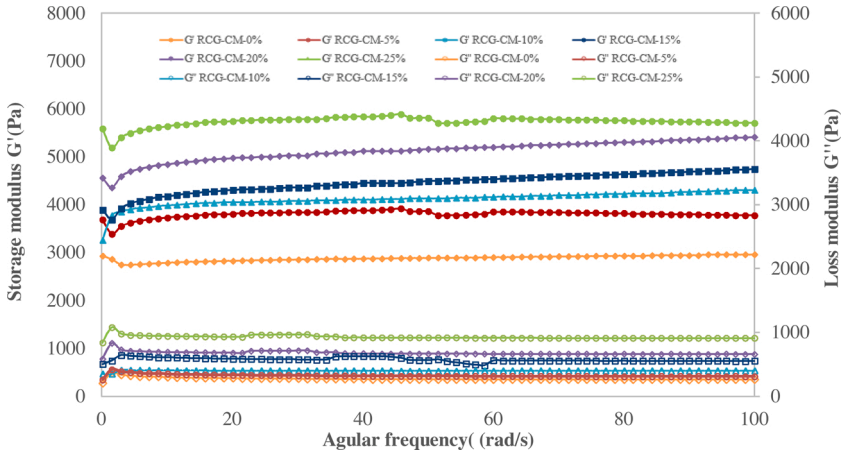


**Fig. 6.** Storage modulus (G′) and loss modulus (G″) of RCG hydrogels reinforced by different CM concentration as a function of angular frequency sweep from 0.1 to 100 rad/s at 37 °C.

vary with the amount of CM. Interestingly, hydrogels prepared with 20 % and 25 % exhibited the highest compressive strength of more than 0.25 MPa with a fracture deformation above 40 %. These findings indicate that the CM content strongly affected the hydrogel mechanical performance. Thus, CM is supposed to perform as additional cross-linking junctions in the composite hydrogel providing mechanical strength thanks to stiffer chains generating stronger pore walls [52,64, 65].

### 3.7. *Rheological properties of hydrogels*

The frequency sweep test provides a good rheological description of how the material will perform during storage and application. It is generally considered that the dynamic viscoelasticity of a polymer liquid at low frequency range is significantly sensitive to structure changes or to the development of a network structure [66]. To effectively evaluate the rheological behavior of composite RCG-CM hydrogels, their storage modulus (G') and loss storage (G'') were determined over a wide range

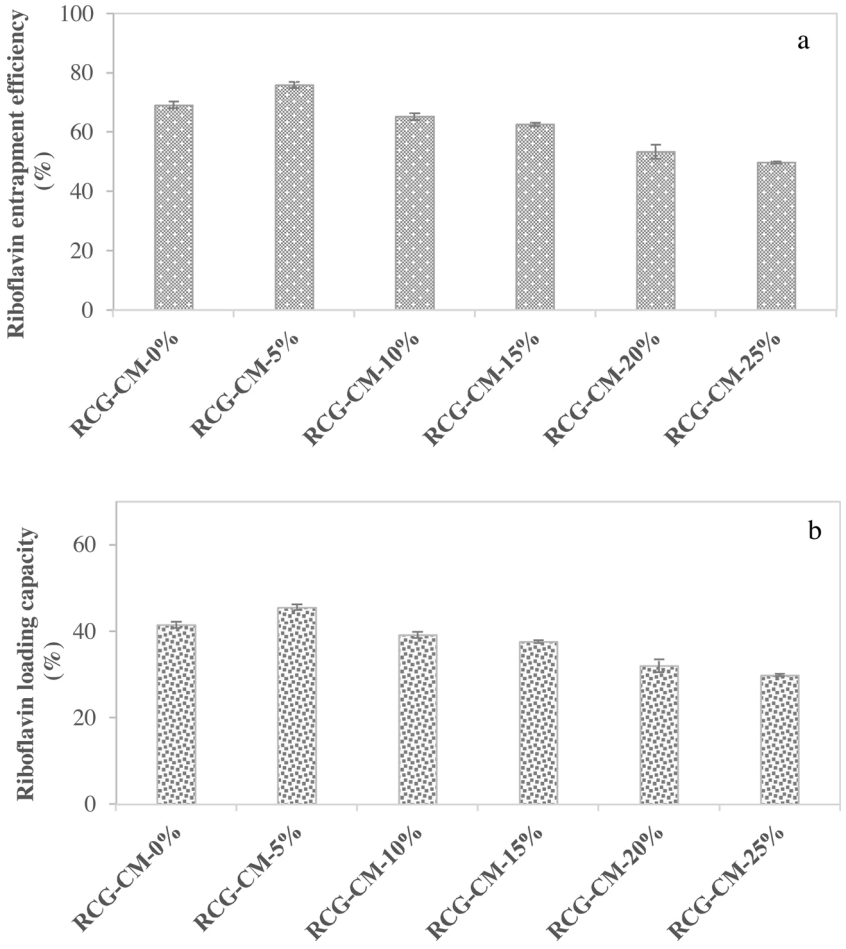


**Fig. 7.** Riboflavin entrapment efficiency (a) and loading capacity (b) of RCG hydrogels reinforced by different CM concentrations.

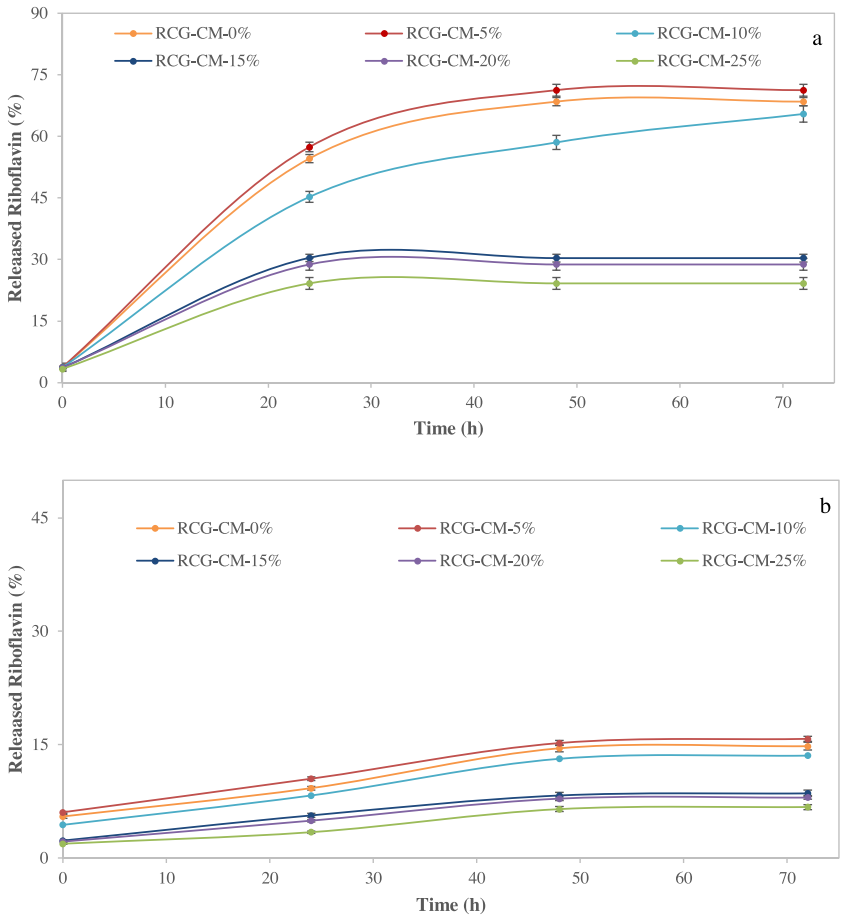


**Fig. 8.** *In vitro* riboflavin release profile and kinetics from RCG-CM hydrogels at pH = 2 (a) and pH = 7.4 (b).

of angular frequencies (0.1–100 rad/s) and results are shown in Fig. 6. The obtained curves showed that all hydrogels exhibited similar rheological behavior. The storage modulus (G') was much higher than the loss modulus (G'') for all hydrogels. This trend proves that crosslinking induced a classic solid-like gel behavior as mentioned by Xu et al. [67] and Alsarra et al. [68]. As shown in Fig. 6, a slightly increase in G' values was perceived for all the hydrogels with a constant slope and independently of the angular frequency, confirming the formation of a fully cured tridimensional network [69,70]. On the other hand, with increasing angular frequency, G'' remained almost unchanged. Hypothetically, uncrosslinked polymer chains have no time to relax at high frequencies. Hence, the elastic energy has been accumulated in polymers, resulting in a high modulus. Nevertheless, the usual relaxing and slipping chain movements are inhibited for cross-linked polymers, ensuring a relatively stable modulus in the measured frequency range [71]. Compared to RCG-CM-0% hydrogel, increasing the CM content from 5 to 25 % led to storage modulus increase, while the loss modulus only slightly changed. This enhancement of storage modulus could be mainly assigned to the energy dissipation mechanism, occasioning a more uniform distribution of CM among the whole network [71]. In the case of the loss modulus, it is more sensitive to molecular motions. The mobility of polymer chains in the three dimensional network is hindered by the filler reinforcement [72]. Thus, the slight variation in G'' values corroborates with the formation of a stiffer structure with lower chain mobility.

### 3.8. *In vitro drug release*

The porous microstructure of hydrogels provides a matching microenvironment to encapsulate drugs, thus slowing their degradation, prolonging their bioavailability, thereby providing prolonged drug release [73]. The Riboflavin entrapment efficiency (EE) and loading capacity (LC) were determined to evaluate the potential of RCG-CM composite hydrogels to serve as drug carrier, as shown in Fig. 7. A maximum Riboflavin EE of 75.8 % was detected for RCG-CM-5% which is higher than that of RCG-CM-0% (69.1 %). However, above 5% of added CM, the EE tends to decrease to reach its minimum (49.7 %) for RCG-CM-25 %. Concerning the LC of Riboflavin, a similar profile was observed, with a maximum LC of 45.5 % for RCG-CM-5% against 41.4 % for RCG-CM-0%. It is of interest to note that both EE and LC changes with CM content are similar to those of swelling ratio. These findings are in accordance with those found by Ooi et al. [21]. In fact, the initial increase in riboflavin encapsulation, for 5% of CM, could be explained by the concomitant rise of the hydrogel swelling ratio permitting to riboflavin an ease entrapment in the available three dimensional network. Meanwhile, the decrease in the amount of encapsulated riboflavin at a concentration exceeding 5% could be due to the gradual saturation of the voids in the gelatin network, resulting in the formation of more stiff hydrogel structure. Thus, it can be concluded that as much as the hydrogel rigidity increased with the addition of CM, a barrier will take place and prevent the entry of drug solution into the network, leading to the decrease in riboflavin loading.

The release profile of riboflavin from RCG based hydrogel was investigated under *in vitro* conditions at pH 2 and pH = 7.4 at 37 °C and results are shown in Fig. 8. All hydrogels display similar release profiles at each pH. At pH 2, an initial fast release is observed during the first 24 h. Beyond, drug release slightly increases to reach 68 %, 71 % and 65 % for RCG-CM-0%, RCG-CM-5%, and RCG-CM-10 %, respectively. In contrast, drug release remained unchanged for RCG-CM-15 %, RCG-CM-20 %, and RCG-CM-25 % beyond 24 h, with a cumulative release of 30

%, 29 % and 24 %, respectively. Indeed, the initial quick release corresponds to that of riboflavin molecules present on the surface of the hydrogel [21]. However, hydrogels loaded by riboflavin and incubated at pH 7.4 displayed lower level of released drug. Precisely, all the hydrogels released the maximum of riboflavin during the first 48 h and remains constant during the following 24 h with 14.8 %, 15.7 %, 13.5 %, 8.5 %, 8% and 6.7 % for hydrogels with a CM concentration from 0% to 25 %. Comparison with Fig. 2 reveals that the rate of drug release was affected by the swelling ratio of the hydrogel in aqueous media which strongly regulate its pore sizes. In fact, hydrogels with higher swelling ratio displayed the biggest pore size, responsible for the easy release of riboflavin leading to the highest drug release rates. Meanwhile, the lower drug release rates for hydrogels with high CM contents could be caused by the network thickness that acted as a diffusion barrier and reduced the pore sizes. Therefore, RCG-CM hydrogels, especially RCG-CM-5% and RCG-CM-10 % can be considered as a promoting carrier for riboflavin delivery because they ensured a good balance between drug loading efficiency and drug release rate.

## 4. Conclusion

In this work, new composite hydrogels were developed from fish gelatin, using cellulose microcrystals as strengthening agent. The composite hydrogels present improved mechanical properties as compared to neat gelatin hydrogel, including stiffness and toughness, improved fraction strain and good recoverability of the initial elastic structure. The properties of RCG-CM hydrogels including pore size, thermal stability, and swelling behavior are dependent on the CM content and pH-sensitive. The highest swelling ratio is obtained at pH 2 due to electrostatic repulsion of protonated amino groups. RCG based hydrogel loaded with 5% of CM exhibits higher swelling ratio than the other hydrogels. Moreover, the SEM micrographs reveal a porous structure for all hydrogels, and the pore size tends to decrease with addition of CM. Riboflavin was successfully loaded in RCG-CM hydrogels by immersion of dried gels in drug solutions. The drug loading and release properties are highly dependent on the swelling ratio of hydrogels. The highest drug loading capacity and entrapment efficiency were obtained for gelatin hydrogel reinforced with 5% CM. Higher drug release rates are also obtained for hydrogels with higher swelling ratios. Therefore, RCG based hydrogels reinforced with CM could be applied as smart pH-sensitive drug carriers.

## CRediT authorship contribution statement

**Soumaya Boughriba:** Conceptualization, Investigation, Writing - original draft. **Nabil Souissi:** Resources, Writing - review & editing, Visualization. **Rim Nasri:** Funding acquisition. **Moncef Nasri:** Project administration. **Suming Li:** Funding acquisition, Writing - review & editing.


## Aknowlegments

This research work was conducted in the framework of PHC-Utique Program, (partenariat Hubert Curien « Utique » du Ministère de l'Europe et des Affaires Etrangères français et du Ministère de l'Enseignement et de la Recherche Scientifique tunisien) financed by CMCU (Comité mixte de coopération universitaire), grant N°: 19G0815.


## References


[1] P. Mokhtari, M. Ghaedi, Water compatible molecularly imprinted polymer for controlled release of riboflavin as drug delivery system, Eur. Polym. J. 118 (2019) 614–618.
[2] M. Barile, T.A. Giancaspero, P. Leone, M. Galluccio, C. Indiveri, Riboflavin transport and metabolism in humans, J. Inherit. Metab. Dis. 39 (4) (2016) 545–557.
[3] A.A. Heikal, Intracellular coenzymes as natural biomarkers for metabolic activities and mitochondrial anomalies, Biomark. Med. 4 (2) (2010) 241–263.
[4] K.C. Reinert, W. Gao, G. Chen, T.J. Ebner, Flavoprotein autofluorescence imaging in the cerebellar cortex in vivo, J. Neurosci. Res. 85 (15) (2007) 3221–3232.
[5] M. Arabi, M. Ghaedi, A. Ostovan, Development of a lower toxic approach based on green synthesis of water-compatible molecularly imprinted nanoparticles for the extraction of hydrochlorothiazide from human urine, ACS Sustain. Chem. Eng. 5 (5) (2017) 3775–3785.
[6] M. Ashoori, A. Saedisomeolia, Riboflavin (vitamin B 2) and oxidative stress: a review, Br. J. Nutr. 111 (11) (2014) 1985–1991.
[7] D. Mehtani, A. Seth, P. Sharma, N. Maheshwari, D. Kapoor, S.K. Shrivastava, R. K. Tekade, Biomaterials for sustained and controlled delivery of small drug molecules. Biomaterials and Bionanotechnology, Elsevier, 2019, pp. 89–152.
[8] D. Bhowmik, H. Gopinath, B.P. Kumar, S. Duraivel, K.S. Kumar, Recent advances in novel topical drug delivery system, Pharma Innov. 1 (9, Part A) (2012) 12.
[9] X. Hu, Y. Wang, L. Zhang, M. Xu, Formation of self-assembled polyelectrolyte complex hydrogel derived from salecan and chitosan for sustained release of Vitamin C, Carbohydr. Polym. 234 (2020), 115920.
[10] B. Massoumi, Z. Mozaffari, M. Jaymand, A starch-based stimuli-responsive magnetite nanohydrogel as de novo drug delivery system, Int. J. Biol. Macromol. 117 (2018) 418–426.
[11] H. Ding, X. Liang, Q. Wang, M. Wang, Z. Li, G. Sun, A semi-interpenetrating network ionic composite hydrogel with low modulus, fast self-recoverability and high conductivity as flexible sensor, Carbohydr. Polym. (2020), 116797.
[12] K. Kaur, R. Jindal, D. Jindal, RSM-CCD optimized microwave-assisted synthesis of chitosan and gelatin-based pH sensitive, inclusion complexes incorporated hydrogels and their use as controlled drug delivery systems, J. Drug Deliv. Sci. Technol. 48 (2018) 161–173.
[13] W. Zhang, X. Jin, H. Li, R. Zhang, C. Wu, Injectable and body temperature sensitive hydrogels based on chitosan and hyaluronic acid for pH sensitive drug release, Carbohydr. Polym. 186 (2018) 82–90.
[14] P. Gupta, K. Vermani, S. Garg, Hydrogels: from controlled release to pH-responsive drug delivery, Drug Discov. Today 7 (10) (2002) 569–579.
[15] I. Kohsari, Z. Shariatinia, S.M. Pourmortazavi, Antibacterial electrospun chitosan-polyethylene oxide nanocomposite mats containing ZIF-8 nanoparticles, Int. J. Biol. Macromol. 91 (2016) 778–788.
[16] C.-J. Lin, C.-H. Kuan, L.-W. Wang, H.-C. Wu, Y. Chen, C.-W. Chang, R.-Y. Huang, T.-W. Wang, Integrated self-assembling drug delivery system possessing dual responsive and active targeting for orthotopic ovarian cancer theranostics, Biomaterials 90 (2016) 12–26.
[17] Z. Shariatinia, Pharmaceutical applications of chitosan, Adv. Colloid Interface Sci. 263 (2019) 131–194.
[18] R. Jahanban-Esfahlan, H. Derakhshankhah, B. Haghshenas, B. Massoumi, M. Abbasian, M. Jaymand, A bio-inspired magnetic natural hydrogel containing gelatin and alginate as a drug delivery system for cancer chemotherapy, Int. J. Biol. Macromol. (2020).
[19] M. Foox, M. Zilberman, Drug delivery from gelatin-based systems, Expert Opin. Drug Deliv. 12 (9) (2015) 1547–1563.
[20] O. Madkhali, G. Mekhail, S.D. Wettig, Modified gelatin nanoparticles for gene delivery, Int. J. Pharm. 554 (2019) 224–234.
[21] S.Y. Ooi, I. Ahmad, M.C.I.M. Amin, Cellulose nanocrystals extracted from rice husks as a reinforcing material in gelatin hydrogels for use in controlled drug delivery systems, Ind. Crops Prod. 93 (2016) 227–234.
[22] K. Yue, G. Trujillo-de Santiago, M.M. Alvarez, A. Tamayol, N. Annabi, A. Khademhosseini, Synthesis, properties, and biomedical applications of gelatin methacryloyl (GelMA) hydrogels, Biomaterials 73 (2015) 254–271.
[23] B.W. Darvell, Materials Science for Dentistry, Woodhead publishing, 2018.
[24] F.A. Andersen, Final report on the safety assessment of glutaral, J. Am. Coll. Toxicol. 15 (2) (1996) 98–139.
[25] S. Farris, K.M. Schaich, L. Liu, P.H. Cooke, L. Piergiovanni, K.L. Yam, Gelatin–pectin composite films from polyion-complex hydrogels, Food Hydrocoll. 25 (1) (2011) 61–70.
[26] Q. Liu, J. Liu, S. Qin, Y. Pei, X. Zheng, K. Tang, High mechanical strength gelatin composite hydrogels reinforced by cellulose nanofibrils with unique beads-on-a-string morphology, Int. J. Biol. Macromol. (2020).
[27] L. Zhou, T. Xu, J. Yan, X. Li, Y. Xie, H. Chen, Fabrication and characterization of matrine-loaded konjac glucomannan/fish gelatin composite hydrogel as antimicrobial wound dressing, Food Hydrocoll. 104 (2020), 105702.
[28] Z. Shariatinia, Biopolymeric nanocomposites in drug delivery. Advanced Biopolymeric Systems for Drug Delivery, Springer, 2020, pp. 233–290.
[29] K. Bethke, S. Palantöken, V. Andrei, M. Roß, V.S. Raghuwanshi, F. Kettemann, K. Greis, T.T.K. Ingber, J.B. Stückrath, S. Valiyaveettil, K. Rademann, Functionalized cellulose for water purification, antimicrobial applications, and sensors, Adv. Funct. Mater. 28 (23) (2018) 1800409, https://doi.org/10.1002/adfm.201800409.
[30] R.J. Moon, A. Martini, J. Nairn, J. Simonsen, J. Youngblood, Cellulose nanomaterials review: structure, properties and nanocomposites, Chem. Soc. Rev. 40 (7) (2011) 3941–3994, https://doi.org/10.1039/C0CS00108B.

[31] M.H. Kim, S. An, K. Won, H.J. Kim, S.H. Lee, Entrapment of enzymes into cellulose–biopolymer composite hydrogel beads using biocompatible ionic liquid, J. Mol. Catal., B Enzym. 75 (2012) 68–72, https://doi.org/10.1016/j.molcatb.2011.11.011.
[32] D. Trache, M.H. Hussin, C.T. Hui Chuin, S. Sabar, M.R.N. Fazita, O.F.A. Taiwo, T. M. Hassan, M.K.M. Haafiz, Microcrystalline cellulose: isolation, characterization and bio-composites application—a review, Int. J. Biol. Macromol. 93 (2016) 789–804, https://doi.org/10.1016/j.ijbiomac.2016.09.056.
[33] S. Boughriba, N. Souissi, M. Jridi, S. Li, M. Nasri, Thermal, mechanical and microstructural characterization and antioxidant potential of Rhinobatos cemiculus gelatin films supplemented by titanium dioxide doped silver nanoparticles, Food Hydrocoll. 103 (2020), 105695, https://doi.org/10.1016/j.foodhyd.2020.105695.
[34] B. Gaihre, S. Aryal, N.A.M. Barakat, H.Y. Kim, Gelatin stabilized iron oxide nanoparticles as a three dimensional template for the hydroxyapatite crystal nucleation and growth, Mater. Sci. Eng. C 28 (8) (2008) 1297–1303, https://doi.org/10.1016/j.msec.2008.01.001.
[35] R. Núñez-Flores, B. Giménez, F. Fernández-Martín, M.E. López-Caballero, M. P. Montero, M.C. Gómez-Guillén, Physical and functional characterization of active fish gelatin films incorporated with lignin, Food Hydrocoll. 30 (1) (2013) 163–172.
[36] I. Yakimets, N. Wellner, A.C. Smith, R.H. Wilson, I. Farhat, J. Mitchell, Mechanical properties with respect to water content of gelatin films in glassy state, Polymer 46 (26) (2005) 12577–12585.
[37] Y. Cao, H. Tan, Structural characterization of cellulose with enzymatic treatment, J. Mol. Struct. 705 (1–3) (2004) 189–193.
[38] N. Annabi, A. Fathi, S.M. Mithieux, P. Martens, A.S. Weiss, F. Dehghani, The effect of elastin on chondrocyte adhesion and proliferation on poly (ε-caprolactone)/elastin composites, Biomaterials 32 (6) (2011) 1517–1525.
[39] M. Contardi, J.A. Heredia-Guerrero, G. Perotto, P. Valentini, P.P. Pompa, R. Spanò, L. Goldoni, R. Bertorelli, A. Athanassiou, I.S. Bayer, Transparent ciprofloxacin-povidone antibiotic films and nanofiber mats as potential skin and wound care dressings, Eur. J. Pharm. Sci. 104 (2017) 133–144.
[40] R.-D. Păvăloiu, A. Stoica-Guzun, T. Dobre, Swelling studies of composite hydrogels based on bacterial cellulose and gelatin, UPB Sci Bull Ser B 77 (2015) 53–62.
[41] O.S. Yin, I. Ahmad, M.C.I.M. Amin, Synthesis of chemical cross-linked gelatin hydrogel reinforced with cellulose nanocrystals (CNC), AIP Conf. Proc. 1614 (1) (2014) 375–380.
[42] L. Gu, T. Li, X. Song, X. Yang, S. Li, L. Chen, P. Liu, X. Gong, C. Chen, L. Sun, Preparation and characterization of methacrylated gelatin/bacterial cellulose composite hydrogels for cartilage tissue engineering, Regen. Biomater. 7 (2) (2020) 195–202.
[43] C.M. Klech, A.P. Simonelli, Examination of the moving boundaries associated with non-Fickian water swelling of glassy gelatin beads: effect of solution pH, J. Memb. Sci. 43 (1) (1989) 87–101.
[44] S. Ge, Q. Liu, M. Li, J. Liu, H. Lu, F. Li, S. Zhang, Q. Sun, L. Xiong, Enhanced mechanical properties and gelling ability of gelatin hydrogels reinforced with chitin whiskers, Food Hydrocoll. 75 (2018) 1–12.
[45] X. Yang, Q. Liu, X. Chen, F. Yu, Z. Zhu, Investigation of PVA/ws-chitosan hydrogels prepared by combined γ-irradiation and freeze-thawing, Carbohydr. Polym. 73 (3) (2008) 401–408.
[46] S. Boral, A.N. Gupta, H.B. Bohidar, Swelling and de-swelling kinetics of gelatin hydrogels in ethanol–water marginal solvent, Int. J. Biol. Macromol. 39 (4–5) (2006) 240–249.
[47] X.J. Yang, P.J. Zheng, Z.D. Cui, N.Q. Zhao, Y.F. Wang, K. De Yao, Swelling behaviour and elastic properties of gelatin gels, Polym. Int. 44 (4) (1997) 448–452.
[48] S. Kim, C.-C. Chu, Pore structure analysis of swollen dextran-methacrylate hydrogels by SEM and mercury intrusion porosimetry, Journal of Biomedical Materials Research: An Official Journal of The Society for Biomaterials, The Japanese Society for Biomaterials, and The Australian Society for Biomaterials and the Korean Society for Biomaterials 53 (3) (2000) 258–266.
[49] H. Liao, H. Zhang, W. Chen, Differential physical, rheological, and biological properties of rapid in situ gelable hydrogels composed of oxidized alginate and gelatin derived from marine or porcine sources, J. Mater. Sci. Mater. Med. 20 (6) (2009) 1263–1271.
[50] D. Rocha-García, A. Guerra-Contreras, J. Reyes-Hernández, G. Palestino, Thermal and kinetic evaluation of biodegradable thermo-sensitive gelatin/poly (ethylene glycol) diamine crosslinked citric acid hydrogels for controlled release of tramadol, Eur. Polym. J. 89 (2017) 42–56.
[51] W. Treesuppharat, P. Rojanapanthu, C. Siangsanoh, H. Manuspiya, S. Ummartyotin, Synthesis and characterization of bacterial cellulose and gelatin-based hydrogel composites for drug-delivery systems, Biotechnol. Rep. 15 (2017) 84–91.
[52] Y. Xie, X. Liao, J. Zhang, F. Yang, Z. Fan, Novel chitosan hydrogels reinforced by silver nanoparticles with ultrahigh mechanical and high antibacterial properties for accelerating wound healing, Int. J. Biol. Macromol. 119 (2018) 402–412.
[53] M. Hamdi, R. Nasri, S. Li, M. Nasri, Bioinspired pH-sensitive riboflavin controlled-release alkaline hydrogels based on blue crab chitosan: study of the effect of polymer characteristics, Int. J. Biol. Macromol. 152 (2020) 1252–1264.
[54] Z. Cai, J. Kim, Preparation and characterization of novel bacterial cellulose/gelatin scaffold for tissue regeneration using bacterial cellulose hydrogel, J. Nanotechnol. Eng. Med. 1 (2) (2010).
[55] N. Halib, M. Amin, I. Ahmad, Physicochemical properties and characterization of nata de coco from local food industries as a source of cellulose, Sains Malays. 41 (2) (2012) 205–211.
[56] O.S. Yin, I. Ahmad, M. Amin, Effect of cellulose nanocrystals content and pH on swelling behaviour of gelatin based hydrogel, Sains Malays. 44 (6) (2015) 793–799.
[57] C. Siangsanoh, S. Ummartyotin, K. Sathirakul, P. Rojanapanthu, W. Treesuppharat, Fabrication and characterization of triple-responsive composite hydrogel for targeted and controlled drug delivery system, J. Mol. Liq. 256 (2018) 90–99, https://doi.org/10.1016/j.molliq.2018.02.026.
[58] S. Maiti, J. Jayaramudu, K. Das, S.M. Reddy, R. Sadiku, S.S. Ray, D. Liu, Preparation and characterization of nano-cellulose with new shape from different precursor, Carbohydr. Polym. 98 (1) (2013) 562–567.
[59] P.G. Gan, S.T. Sam, M.Fbin Abdullah, M.F. Omar, Thermal properties of nanocellulose-reinforced composites: a review, J. Appl. Polym. Sci. 137 (11) (2020) 48544.
[60] I. Jankowska, R. Pankiewicz, K. Pogorzelec-Glaser, P. Lawniczak, A. Lapiński, J. Tritt-Goc, Comparison of structural, thermal and proton conductivity properties of micro-and nanocelluloses, Carbohydr. Polym. 200 (2018) 536–542.
[61] W. Wei, J. Li, X. Qi, Y. Zhong, G. Zuo, X. Pan, T. Su, J. Zhang, W. Dong, Synthesis and characterization of a multi-sensitive polysaccharide hydrogel for drug delivery, Carbohydr. Polym. 177 (2017) 275–283.
[62] V.N. Izmailova, S.R. Derkach, M.A. Sakvarelidze, S.M. Levachev, K. VORON, Gelation in gelatin and gelatin-containing multicomponent blends, Polym. Sci. Ser. C 46 (2004) 73–92.
[63] M.Mde S. Lima, R. Borsali, Rodlike cellulose microcrystals: structure, properties, and applications, Macromol. Rapid Commun. 25 (7) (2004) 771–787, https://doi.org/10.1002/marc.200300268.
[64] Z. Naghizadeh, A. Karkhaneh, A. Khojasteh, Self-crosslinking effect of chitosan and gelatin on alginate based hydrogels: injectable in situ forming scaffolds, Mater. Sci. Eng. C 89 (2018) 256–264, https://doi.org/10.1016/j.msec.2018.04.018.
[65] F. Wang, Y. Wen, T. Bai, The composite hydrogels of polyvinyl alcohol–gellan gum-Ca2+ with improved network structure and mechanical property, Mater. Sci. Eng. C 69 (2016) 268–275, https://doi.org/10.1016/j.msec.2016.06.084.
[66] O. Zandraa, L. Jelínková, N. Roy, T. Sáha, T. Kitano, N. Saha, Viscoelastic properties and morphology of mumio-based medicated hydrogels, AIP Conf. Proc. 1375 (1) (2011) 261–271, https://doi.org/10.1063/1.3604487.
[67] Y. Xu, Q. Wu, Y. Sun, H. Bai, G. Shi, Three-dimensional self-assembly of graphene oxide and DNA into multifunctional hydrogels, ACS Nano 4 (12) (2010) 7358–7362.
[68] I.A. Alsarra, A.Y. Hamed, F.K. Alanazi, S.H. Neau, Rheological and mucoadhesive characterization of poly (vinylpyrrolidone) hydrogels designed for nasal mucosal drug delivery, Arch. Pharm. Res. 34 (4) (2011) 573.
[69] G. Pitarresi, D. Giacomazza, D. Triolo, G. Giammona, P.L. San Biagio, Rheological characterization and release properties of inulin-based hydrogels, Carbohydr. Polym. 88 (3) (2012) 1033–1040.
[70] P.D. Williams, M.H. Oztop, M.J. McCarthy, K.L. McCarthy, Y.M. Lo, Characterization of water distribution in xanthan-curdlan hydrogel complex using magnetic resonance imaging, nuclear magnetic resonance relaxometry, rheology, and scanning Electron microscopy, J. Food Sci. 76 (6) (2011) E472–E478, https://doi.org/10.1111/j.1750-3841.2011.02227.x.
[71] B. Chen, X. Hu, An injectable composite gelatin hydrogel with pH response properties, . 2017 (2017).
[72] P.S. Nagendra, V.V.S. Prasad, K. Ramji, A study on dynamic mechanical analysis of natural nano banana particle filled polymer matrix composites, Mater. Today Proc. 4 (8) (2017) 9081–9086.
[73] C.A. Dreiss, Hydrogel design strategies for drug delivery, Curr. Opin. Colloid Interface Sci. (2020).